Dalton Transactions

ROYAL SOCIETY OF CHEMISTRY

PAPER

View Article Online
View Journal | View Issue

Cite this: *Dalton Trans.*, 2025, **54**, 12818

The constitutional dynamic chemistry of Au_3(pyrazolate)$_3$ complexes

Noga Eren, Renata Svecova, Farzaneh Fadaei-Tirani, Rosario Scopelliti and Kay Severin *

Received 9th July 2025,
Accepted 4th August 2025

DOI: 10.1039/d5dt01613d

rsc.li/dalton

Trinuclear $Au_3(Pz)_3$ complexes (Pz = pyrazolate) have been used extensively as components in molecular and polymeric nanostructures. However, the constitutional dynamic chemistry of $Au_3(Pz)_3$ complexes remains largely unexplored. We have investigated exchange reactions between $Au_3(Pz)_3$ complexes and pyrazole ligands in homogeneous solution. At room temperature and at low millimolar concentrations, several days were needed to establish the thermodynamic equilibrium. The slow exchange kinetics corroborate the inert character of $Au_3(Pz)_3$ complexes. When 3,5-diisopropylpyrazolato or 3,5-diphenylpyrazolato ligands were replaced by 3,5-bis(trifluoromethyl)pyrazolato ligands, a sigmoidal rate profile was observed. This observation led to the discovery that pyrazoles can act as potent (auto)catalysts for ligand exchange and ligand scrambling reactions with $Au_3(Pz)_3$ complexes. The kinetic studies were supplemented by crystallographic analyses of four heteroleptic $Au_3(Pz)_2(Pz')$ complexes.

Introduction

Trinuclear gold(I) complexes with bridging pyrazolate ligands represent versatile building blocks for metallosupramolecular chemistry and materials science.[1] $Au_3(Pz)_3$ complexes (Pz = pyrazolate) are easily accessible by combining pyrazoles with AuClL (L = SMe_2 or tetrahydrothiophene) in the presence of base.[1,2] The synthetic procedure is compatible with a wide range of substituents at the heterocycle, including functional groups such as aldehydes,[3] carboxylic acids,[4] thiophenes,[5] and pyridines.[6] $Au_3(Pz)_3$ complexes are prone to aggregate *via* aurophilic interactions, and the resulting assemblies are often luminescent.[1] Moreover, $Au_3(Pz)_3$ complexes can display pronounced π-basicity,[7] promoting the interaction with π-acidic compounds[8] or with metal ions.[4,9]

$Au_3(Pz)_3$ complexes have been investigated in soft matter chemistry. Non-covalent assemblies of $Au_3(Pz)_3$ complexes were found to form liquid crystals,[10] organogels,[11] fibers,[12] or multilayer vesicles ('nano onions').[13] Some of these assemblies are luminescent, and stimuli-controlled emission changes have been explored.[11]

Molecularly defined nanostructures with cage-like architectures were obtained by combining Au^I complexes with bridged pyrazole ligands,[14] or by linking pre-formed $Au_3(Pz)_3$ complexes *via* metal–ligand interactions[15] or dynamic covalent imine chemistry.[3] The tetrahedral cage **A** (Fig. 1b), for example, was obtained by condensation of tris(2-aminoethyl) amine with a $Au_3(Pz)_3$ complex featuring pendant phenylaldehyde groups. This cage acts as a potent receptor for C_{60} and C_{70}.[3]

$Au_3(Pz)_3$ complexes have also been used for the construction of polymeric framework materials (Fig. 1c).[16–18] Materials of this type were employed as catalysts for the carboxylation of alkynes with CO_2 [16] or, in combination with Au nanoparticles, as photocatalysts for H_2 evolution.[17]

Metal–ligand exchange reactions are of key importance for the successful construction of metallosupramolecular structures. When the metal–ligand bonds are too inert, error correction processes are suppressed, resulting in the formation of side products. For example, $[PtL_4]^{2+}$ complexes (L = N-donor ligand) are more inert than the analogous $[PdL_4]^{2+}$ complexes, making the construction of $[PtL_4]^{2+}$-based metallosupramolecular structures significantly more challenging.[19]

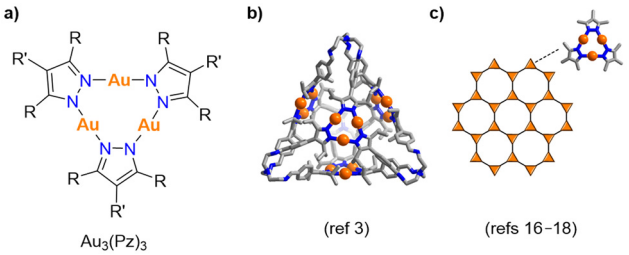

Fig. 1 The general structure of $Au_3(Pz)_3$ complexes (a) and graphic representations of a molecular cage (b) and polymeric networks (c) containing $Au_3(Pz)_3$ complexes.

Institut des Sciences et Ingénierie Chimiques, École Polytechnique Fédérale de Lausanne (EPFL), 1015 Lausanne, Switzerland. E-mail: kay.severin@epfl.ch

Thus far, there is only limited knowledge about the constitutional dynamic chemistry of $Au_3(Pz)_3$ complexes. While synthesizing a $Au_3(Pz)_3$-containing coordination cage, we noticed that heteroleptic complexes of type $Au_3(Pz)_2(Pz')$ do not undergo fast ligand scrambling. The apparent inert character of the Au trimer is in contrast to what was reported for pyrazolate complexes of Cu^I and Ag^I, which can form rapid dynamic equilibria in solution.[20,21]

Below, we describe ligand exchange reactions of $Au_3(Pz)_3$ complexes. Surprisingly, exchange reactions between $Au_3(Pz)_3$ trimers and 'free' pyrazole ligands can display pronounced autocatalytic behavior. This finding led to the discovery that pyrazoles can act as catalysts for ligand exchange and ligand scrambling reactions with $Au_3(Pz)_3$ complexes. To supplement the kinetic studies, crystallographic analyses of four heteroleptic $Au_3(Pz)_2(Pz')$ complexes were performed.

Results and discussion

Ligand exchange reactions

For our investigations, we used the pyrazole ligands depicted in Fig. 2. The corresponding $Au_3(Pz)_3$ complexes were obtained by mixing equimolar amounts of the ligands with $AuCl(SMe_2)$ in the presence of base.[22]

First, we studied ligand exchange between $Au_3(Pz^{Pr})_3$ and $H\text{–}Pz^{CF_3}$. The fluorinated pyrazole ligand $H\text{–}Pz^{CF_3}$ was chosen because the formation of heteroleptic complexes can also be monitored by ^{19}F NMR spectroscopy. A $C_2D_2Cl_4$ solution containing $Au_3(Pz^{Pr})_3$ (4 mM) and $H\text{–}Pz^{CF_3}$ (12 mM) was heated to 60 °C. After 24 h, the thermal equilibrium was reached. NMR spectroscopy indicated the presence of three main complexes: $Au_3(Pz^{Pr})_3$ (40%), $Au_3(Pz^{Pr})_2(Pz^{CF_3})$ (51%), and $Au_3(Pz^{Pr})(Pz^{CF_3})_2$ (9%) (Scheme 1). The homotrimer $Au_3(Pz^{CF_3})_3$ was not detected in significant amounts (<3%). As expected, a similar equilibrium distribution was observed for the 'inverse' reaction between $Au_3(Pz^{CF_3})_3$ and $H\text{–}Pz^{Pr}$ (see the SI, Fig. S33 and S34). From these experiments, one can conclude that: (a) ligand exchange is possible but slow, and (b) excess ligand does not compromise the stability of $Au_3(Pz)_3$ trimers to a significant extent, and (c) Pz^{Pr}-containing Au trimers are more stable than Pz^{CF_3}-containing trimers.

A similar ligand exchange reaction was performed using toluene-d_8 instead of $C_2D_2Cl_4$ as the solvent. The reaction was slower, and 3 days were required to reach the equilibrium. The spectra of the equilibrated mixture revealed the presence of two trinuclear complexes: $Au_3(Pz^{Pr})_3$ (61%), $Au_3(Pz^{Pr})_2(Pz^{CF_3})$ (39%). These results show that the nature of the solvent can influence the equilibrium distribution substantially. A possible factor for the altered distribution is a solvent effect on the relative stability of $H\text{–}Pz^{Pr}$ and $H\text{–}Pz^{CF_3}$. Pyrazoles are known to self-aggregate *via* hydrogen bonding,[23] and the stability of these aggregates is expected to depend on the nature of the solvent and on the substituents on the pyrazole.

An unexpected finding was the sigmoidal rate profile for the ligand exchange reactions in both $C_2D_2Cl_4$ and in toluene-d_8 (Fig. 3, traces in blue). To further investigate this unusual kinetic behavior, we performed a kinetic study in $C_2D_2Cl_4$ at room temperature.

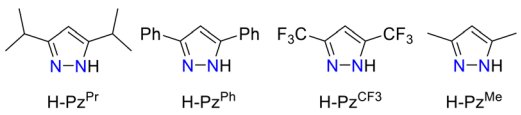

Fig. 2 Structure of the ligands used in this study.

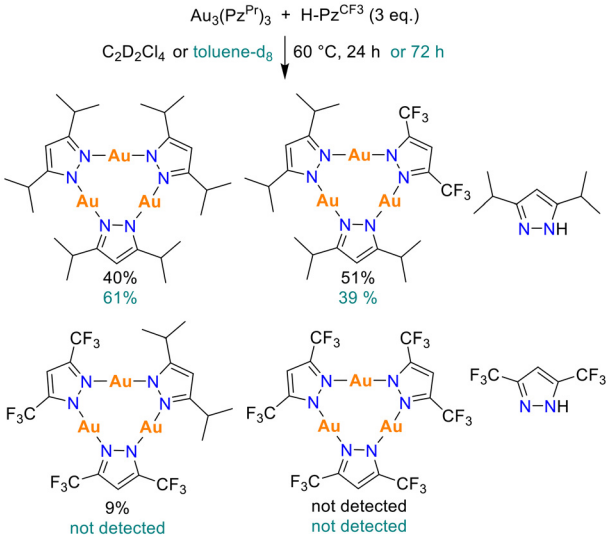

Scheme 1 Reaction between $Au_3(Pz^{Pr})_3$ (4 mM) and $H\text{–}Pz^{CF_3}$ (12 mM) in either $C_2D_2Cl_4$ or toluene-d_8 and the product distribution after equilibration.

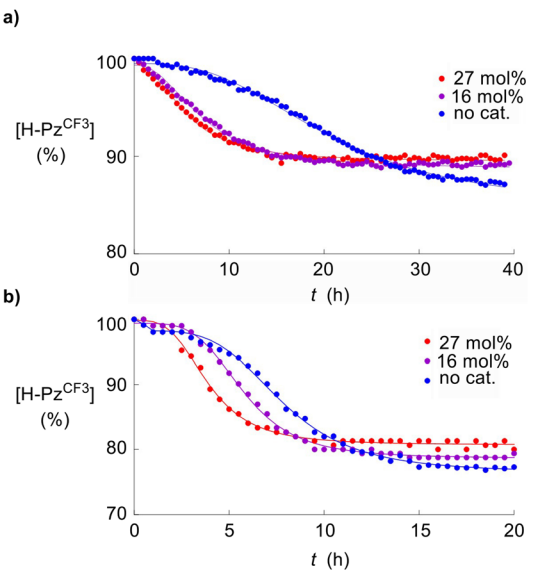

Fig. 3 Conversion of $H\text{–}Pz^{CF_3}$ *versus* time in reactions of $Au_3(Pz^{Pr})_3$ (4 mM) with $H\text{–}Pz^{CF_3}$ (12 mM) at 60 °C in the presence of 0 mol% (blue circles), 16 mol% (purple circles), 27 mol% (red circles) of $H\text{–}Pz^{Pr}$ (with respect to $Au_3(Pz^{Pr})_3$) in toluene-d_8 (a) or in $C_2D_2Cl_4$ (b).

^{1}H NMR spectroscopic monitoring of the reaction at RT confirmed the presence of a pronounced induction period (see the SI, Fig. S39). For the first 200 h, the concentration of H–Pz^{CF_3} diminished by only 4%. Subsequently, a rapid decrease of the H–Pz^{CF_3} concentration was observed until its concentration approached the equilibrium distribution.

Sigmoidal rate profiles are a typical characteristic of autocatalytic reactions.[24] The presence of an autocatalytic system can be corroborated by enhanced reaction kinetics in the presence of externally added products. The reaction between $Au_3(Pz^{Pr})_3$ and H–Pz^{CF_3} produces two new Au trimers along with H–Pz^{Pr}. The latter appeared to be the most likely candidate for a potential catalyst. Therefore, we repeated the reaction between $Au_3(Pz^{Pr})_3$ and H–Pz^{CF_3} in the presence of different amounts of H–Pz^{Pr} (16 or 27 mol% with respect to the Au-trimer), both in toluene-d_8 and in $C_2D_2Cl_4$. Significant rate enhancements were observed in the presence of H–Pz^{Pr} (Fig. 3). As expected, the presence of H–Pz^{Pr} also shifted the equilibrium distribution of the complexes, with more remaining H–Pz^{CF_3} in the presence of H–Pz^{Pr}.

The results described above show that H–Pz^{Pr} can act as a catalyst, but not H–Pz^{CF_3}. The latter pyrazole ligand is significantly less basic than H–Pz^{Pr}: the calculated pK_a of protonated (H–Pz^{CF_3}–H)$^+$ is 0.17, whereas a value of 3.70 was calculated for (H–Pz^{Pr}–H)$^+$.[25] On the other hand, the neutral ligand H–Pz^{CF_3} (pK_a = 9.57) is more acidic than H–Pz^{Pr} (pK_a = 15.08). Assuming a correlation between ligand basicity and ligand donor strength, H–Pz^{CF_3} is expected to be a worse ligand than H–Pz^{Pr}, both in the neutral and in the deprotonated form.

A plausible explanation for the autocatalytic behavior in the reaction between $Au_3(Pz^{Pr})_3$ and H–Pz^{CF_3} is that ligand exchange proceeds *via* an associative mechanism, with initial formation of an adduct between $Au_3(Pz^{Pr})_3$ and H–Pz^{Pr}. The adduct then undergoes fast ligand exchange with H–Pz^{CF_3} to give $Au_3(Pz^{Pr})_2(Pz^{CF_3})$ and the regenerated catalysts H–Pz^{Pr}.

Attempts to detect an adduct between $Au_3(Pz^{Pr})_3$ and H–Pz^{Pr} spectroscopically were not successful. The ^{1}H NMR spectrum of an equimolar mixture of $Au_3(Pz^{Pr})_3$ (4 mM) and H–Pz^{Pr} (12 mM) in toluene-d_8 after equilibration for 24 h showed neither signals of a new complex nor significant shifts when compared to the spectra of the individual compounds (see the SI, Fig. S32). The proposed intermediate is therefore not formed in larger amounts.

Analogous exchange reactions were then performed with $Au_3(Pz^{Ph})_3$ and three equivalents of H–Pz^{CF_3} ($C_2D_2Cl_4$, RT, Scheme 2). The ^{19}F NMR spectrum of the equilibrated reaction mixture indicated the formation of two main new complexes, which can be assigned as the heteroleptic complexes $Au_3(Pz^{Ph})_2(Pz^{CF_3})$ (45%) and $Au_3(Pz^{Ph})(Pz^{CF_3})_2$ (26%). As in the case of $Au_3(Pz^{Pr})_3$, the rate profile displayed an induction period. However, the reaction was overall faster, with equilibrium being established after ~10 hours. The faster ligand exchange for reactions involving $Au_3(Pz^{Ph})_3$ instead of $Au_3(Pz^{Pr})_3$ likely reflects a lower relative stability of the former trimer. A pronounced rate enhancement was observed when

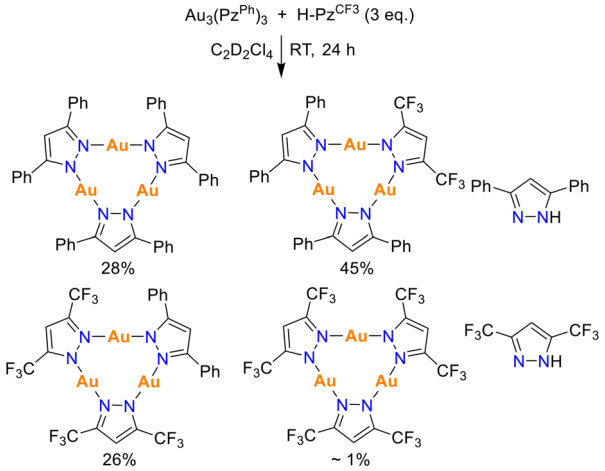

Scheme 2 Reaction between $Au_3(Pz^{Ph})_3$ (4 mM) and H–Pz^{CF_3} (12 mM) and the product distribution after equilibration.

the reaction was performed in the presence of 30 mol% of H–Pz^{Ph}, indicating again an autocatalytic behavior (Fig. 4).

Next, we studied ligand exchange reactions between two trimeric complexes, $Au_3(Pz^{Pr})_3$ and $Au_3(Pz^{Ph})_3$. Ligand scrambling was expected to give four complexes, the heteroleptic complexes $Au_3(Pz^{Ph})_2(Pz^{Pr})$ and $Au_3(Pz^{Ph})(Pz^{Pr})_2$ along with the homotrimers $Au_3(Pz^{Pr})_3$ and $Au_3(Pz^{Ph})_3$ (Scheme 3). For monitoring the reaction, we used *in situ* ^{1}H NMR spectroscopy. The three complexes containing Pz^{Ph} ligands show well-resolved signals for the aromatic C–H atoms of the heterocycle at 6.98–7.04 ppm.

As expected, ligand scrambling in $C_2D_2Cl_4$ at RT was very slow. After 208 h, only 6.5% of $Au_3(Pz^{Ph})_3$ had converted into new complexes (Scheme 3 and SI, Fig. S54). When 30 mol% of the 'free' pyrazole ligand H–Pz^{Ph} was added to the reaction mixture, a pronounced rate enhancement was observed (32% conversion). A similar rate enhancement was noted for reactions in the presence of H–Pz^{Pr} (33% conversion). An inspection of the ^{1}H NMR spectra showed that H–Pz^{Pr} got incorporated into the Au trimers, with liberation of H–Pz^{Ph} (see the SI, Fig. S50). The latter pyrazole then takes over the role as the catalyst. Attempts to use other N-donors such as pyridine or

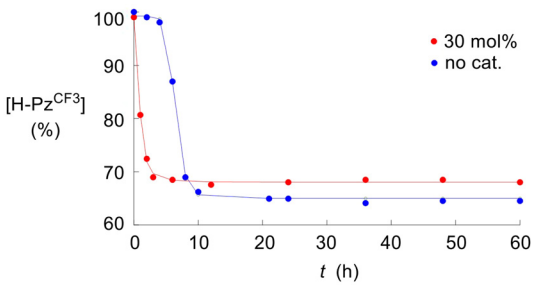

Fig. 4 Conversion of H–Pz^{CF_3} *versus* time in reactions of $Au_3(Pz^{Ph})_3$ (4 mM) with H–Pz^{CF_3} (12 mM) in the presence of 0 mol% (blue circles) and 30 mol% (red circles) of H–Pz^{Ph} (with respect to $Au_3(Pz^{Ph})_3$).

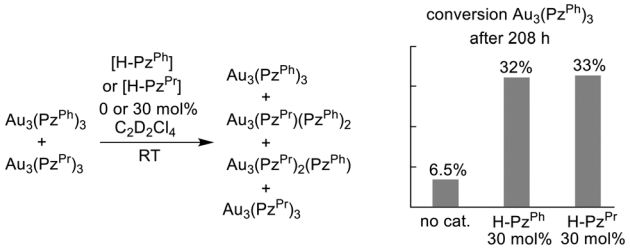

Scheme 3 Reaction between $Au_3(Pz^{Ph})_3$ (4.1 mM) and $Au_3(Pz^{Pr})_3$ (4 mM) in the absence or in the presence of the catalysts H–Pz^{Ph} or H–Pz^{Pr} (30 mol% each), and the conversion of $Au_3(Pz^{Ph})_3$ after 208 h (right side).

1-isopropylimidazole as catalysts led to partial decomposition of the gold trimers and to the formation of Au nanoparticles.

Crystallographic investigations

Thus far, structural investigations of gold pyrazolate complexes have focused on homoleptic complexes of type $Au_3(Pz)_3$.[1] To complement our kinetic investigations, we have analyzed the structures of four heteroleptic $Au_3(Pz)_2(Pz')$ complexes by single-crystal X-ray diffraction (XRD).

The targeted synthesis of $Au_3(Pz)_2(Pz')$ complexes from the corresponding precursors was found to be difficult because mixtures of complexes were typically obtained. An exception was the heteroleptic trimer $Au_3(Pz^{Ph})_2(Pz^{CF_3})$, which could be isolated on a preparative scale in low yield (20%) by combining $AuCl(SMe_2)$ with a mixture of H–Pz^{Ph} and H–Pz^{CF_3} in methanol in the presence of NEt_3 (for details, see the SI, section 2.2). Crystals of heteroleptic complexes containing Pz^{Me} were obtained by combining toluene solutions of the homoleptic complexes $Au_3(Pz^{Ph})_3$ or $Au_3(Pz^{CF_3})_3$ with a toluene solution of H–Pz^{Me}.

The molecular structures of $Au_3(Pz^{Ph})_2(Pz^{CF_3})$, $Au_3(Pz^{Me})_2(Pz^{Ph})$, $Au_3(Pz^{Me})_2(Pz^{CF_3})$, and $Au_3(Pz^{CF_3})_2(Pz^{Me})$, as determined by single-crystal XRD, are depicted in Fig. 5. Key structural parameters for the four complexes are summarized in the SI, Tables S1–S4.

The presence of two different ligands does not result in a desymmetrization of the central nine-membered $(Au–N–N)_3$ ring system. The Au(I) centers in the four complexes all show a nearly perfect linear coordination geometry ($\alpha_{N–Au–N}$: 174.98–179.88°), and the Au–N bond distances are all within a narrow range (1.964–2.040 Å).

All four heteroleptic $Au_3(Pz)_2(Pz')$ complexes display intermolecular Au···Au contacts in the solid state (Fig. 5, graphics on the right side). Crystalline $Au_3(Pz^{Ph})_2(Pz^{CF_3})$ features isolated pairs of co-planar trimers with Au···Au distances of 3.3065(7) and 3.3415(7) Å. The central $(Au–N–N)_3$ rings are arranged in an eclipsed fashion,[26] with the Pz^{CF_3} ligand of one trimer facing a Pz^{Ph} ligand of an adjacent trimer. The close Au···Au contacts observed for $Au_3(Pz^{Ph})_2(Pz^{CF_3})$ are in contrast to the structure of the homoleptic complex $Au_3(Pz^{Ph})_3$, which does not show intermolecular Au···Au interactions in the solid state.[27]

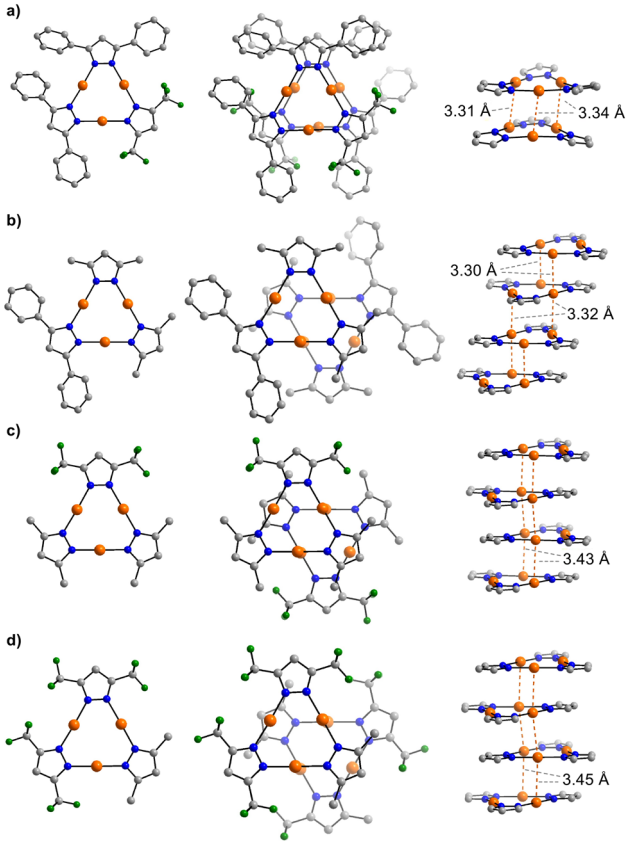

Fig. 5 Molecular structures and the stacking of the heteroleptic complexes $Au_3(Pz^{Ph})_2(Pz^{CF_3})$ (a), $Au_3(Pz^{Me})_2(Pz^{Ph})$ (b), $Au_3(Pz^{Me})_2(Pz^{CF_3})$ (c), and $Au_3(Pz^{CF_3})_2(Pz^{Me})$ (d) in the crystal. Color coding: C gray, N blue, Au orange, F green. Hydrogen atoms are not shown for clarity. For the graphics on the right, the side chains (Ph, Me, or CF_3) are omitted.

The three other heteroleptic complexes $Au_3(Pz^{Me})_2(Pz^{Ph})$, $Au_3(Pz^{Me})_2(Pz^{CF_3})$, and $Au_3(Pz^{CF_3})_2(Pz^{Me})$ all show a columnar arrangement of co-planar Au trimers. The individual complexes are linked *via* two close Au···Au contacts.

Conclusions

The constitutional dynamic chemistry of $Au_3(Pz)_3$ complexes was investigated. Ligand exchange reactions were found to be slow, requiring several days to reach thermodynamic equilibrium. These results highlight the inert nature of $Au_3(Pz)_3$ complexes. The displacement of Pz^{Pr} or Pz^{Ph} ligands with Pz^{CF_3} ligands resulted in sigmoidal rate profiles. Subsequent studies revealed that pyrazoles can function as potent (auto)catalysts in ligand exchange and ligand scrambling reactions. The kinetic studies were supplemented by crystallographic analyses of four heteroleptic $Au_3(Pz)_2(Pz')$ complexes.

Our result should be considered when using $Au_3(Pz)_3$ complexes for the construction of supramolecular architectures.

On one hand, error correction processes may be compromised by the inert character of $Au_3(Pz)_3$ complexes. On the other hand, it would be possible to facilitate thermal equilibration processes by using pyrazoles as catalysts.

Author contributions

N. E. and R. S. performed the experiments and analyzed the data, F. F.-T. and R. S. collected and processed the X-ray data, and N. E. and K. S. co-wrote the manuscript. All authors discussed the results and commented on the manuscript.

Conflicts of interest

There are no conflicts to declare.

Data availability

The data supporting this article have been included as part of the SI: synthetic procedures and experimental details. See DOI: **https://doi.org/10.1039/d5dt01613d**.

CCDC 2453718, 2453719, 2453717 and 2440472 contains the supplementary crystallographic data for this paper.[28a–d]

Acknowledgements

The work was supported by the école Polytechnique Fédérale de Lausanne (EPFL).

References

1 For review articles, see: (*a*) J. Zheng, Z. Lu, K. Wu, G.-H. Ning and D. Li, *Chem. Rev.*, 2020, **120**, 9675–9742; (*b*) R. Galassi, M. A. Rawashdeh-Omary, H. V. R. Dias and M. A. Omary, *Comments Inorg. Chem.*, 2019, **39**, 287–348; (*c*) J. Zheng, H. Yang, M. Xie and D. Li, *Chem. Commun.*, 2019, **55**, 7134–7146; (*d*) M. A. Omray, A. A. Mohamed, M. A. Rawashdeh-Omary and J. P. Fackler Jr., *Coord. Chem. Rev.*, 2005, **249**, 1372–1381; (*e*) A. Burini, A. A. Mohamed and J. P. Fackler, *Comments Inorg. Chem.*, 2003, **24**, 253–280.

2 For pioneering studies, see: (*a*) G. Minghetti, G. Banditelli and F. Bonati, *Inorg. Chem.*, 1979, **18**, 658–663; (*b*) F. Bonati, G. Minghetti and G. Banditelli, *J. Chem. Soc., Chem. Commun.*, 1974, 88–89.

3 N. Eren, F. Fadaei-Tirani, R. Scopelliti and K. Severin, *Chem. Sci.*, 2024, **15**, 3539–3544.

4 P. K. Upadhyay, S. B. Marpu, E. N. Benton, C. L. Williams, A. Telang and M. A. Omary, *Anal. Chem.*, 2018, **90**, 4999–5006.

5 L. D. Early, J. K. Nagle and M. O. Wolf, *Inorg. Chem.*, 2014, **53**, 7106–7117.

6 T. Osuga, T. Murase, M. Hoshino and M. Fujita, *Angew. Chem., Int. Ed.*, 2014, **53**, 11186–11189.

7 S. M. Tekarli, T. R. Cundari and M. A. Omary, *J. Am. Chem. Soc.*, 2008, **130**, 1669–1675.

8 Z. Lu, B. Chilukuri, C. Yang, A.-M. M. Rawashdeh, R. K. Arvapally, S. M. Tekarli, X. Wang, C. T. Cardenas, R. R. Cundari and M. A. Omary, *Chem. Sci.*, 2020, **11**, 11179–11188.

9 (*a*) Z. Lu, Y.-J. Yang, W.-X. Ni, M. Li, Y. Zhao, Y.-L. Huang, D. Luo, X. Wang, M. A. Omary and D. Li, *Chem. Sci.*, 2021, **12**, 702–708; (*b*) W.-X. Ni, Y.-M. Qiu, M. Li, J. Zheng, R. W.-Y. Sun, S.-Z. Zhan, S. W. Ng and D. Li, *J. Am. Chem. Soc.*, 2014, **136**, 9532–9535; (*c*) H. O. Lintang, K. Kinbara, T. Yamashita and T. Aida, *Chem. – Asian J.*, 2012, **7**, 2068–2072; (*d*) T. Osuga, T. Murase and M. Fujita, *Angew. Chem., Int. Ed.*, 2012, **51**, 12199–12201.

10 (*a*) E. Beltrán, J. Barberá, J. L. Serrano, A. Elduque and R. Giménez, *Eur. J. Inorg. Chem.*, 2014, 1165–1173; (*b*) H. O. Lintang, K. Kinbara, K. Tanaka, T. Yamashita and T. Aida, *Angew. Chem., Int. Ed.*, 2010, **49**, 4241–4245; (*c*) M. C. Torralba, P. Ovejero, M. J. Mayoral, M. Cano, J. A. Campo, J. V. Heras, E. Pinilla and M. R. Torres, *Helv. Chim. Acta*, 2004, **87**, 250–263; (*d*) S. J. Kim, S. H. Kang, K.-M. Park, H. Kim, W.-C. Zin, M.-G. Choi and K. Kim, *Chem. Mater.*, 1998, **10**, 1889–1893; (*e*) J. Barberá, A. Elduque, R. Giménez, F. J. Lahoz, J. A. López, L. A. Oro and J. L. Serrano, *Inorg. Chem.*, 1998, **37**, 2960–2967; (*f*) J. Barberá, A. Elduque, R. Gimenez, L. A. Oro and J. L. Serrano, *Angew. Chem., Int. Ed. Engl.*, 1996, **35**, 2832–2835.

11 A. Kishimura, T. Yamashita and T. Aida, *J. Am. Chem. Soc.*, 2005, **127**, 179–183.

12 M. Enomoto, A. Kishimura and T. Aida, *J. Am. Chem. Soc.*, 2001, **123**, 5608–5609.

13 A. B. Solea, D. Dermutas, F. Fadaei-Tirani, L. Leanza, M. Delle Piane, G. M. Pavan and K. Severin, *Nanoscale*, 2025, **17**, 1007–1012.

14 (*a*) M. Veronelli, S. Dechert, A. Schober, S. Demeshko and F. Meyer, *Eur. J. Inorg. Chem.*, 2017, 446–453; (*b*) M. Veronelli, S. Dechert, S. Demeshko and F. Meyer, *Inorg. Chem.*, 2015, **54**, 6917–6927; (*c*) T. Jozak, Y. Sun, Y. Schmitt, S. Lebedkin, M. Kappes, M. Gerhards and W. R. Thiel, *Chem. – Eur. J.*, 2011, **17**, 3384–3389.

15 N. Eren, F. Fadaei-Tirani and K. Severin, *Inorg. Chem. Front.*, 2024, **11**, 3263–3269.

16 R.-J. Wei, M. Xie, R.-Q. Xia, J. Chen, H.-J. Hu, G.-H. Ning and D. Li, *J. Am. Chem. Soc.*, 2023, **145**, 22720–22727.

17 X. Zhu, H. Miao, Y. Shan, G. Gao, Q. Gu, Q. Xiao and X. He, *Inorg. Chem.*, 2022, **61**, 13591–13599.

18 H.-Y. Wang, J.-W. Ye, X.-W. Zhang, C. Wang, D.-Y. Lin, D.-D. Zhou and J.-P. Zhang, *Sci. Bull.*, 2022, **67**, 1229–1232.

19 For a recent publication, see:Z. T. Avery, M. G. Gardiner and D. Preston, *Angew. Chem., Int. Ed.*, 2025, **64**, e202418079.

20 For dynamic CuI pyrazolate complexes, see: (*a*) M. R. Patterson and H. V. R. Dias, *Dalton Trans.*, 2022,

51, 375–383; (*b*) J.-H. Chen, D. Wei, G. Yang, J.-G. Ma and P. Cheng, *Dalton Trans.*, 2020, **49**, 1116–1123; (*c*) H. V. R. Dias, H. V. K. Diyabalanage, M. M. Ghimire, J. M. Hudson, D. Parasar, C. S. P. Gamage, S. Li and M. A. Omary, *Dalton Trans.*, 2019, 14979–14983; (*d*) M. Veronelli, N. Kindermann, S. Dechert, S. Meyer and F. Meyer, *Inorg. Chem.*, 2014, **53**, 2333–2341.

21 (*a*) I. Alkorta, M. T. Benito, J. Elguero, E. G. Doyagüez, M. R. Patterson, M. L. Jimeno, H. V. R. Dias and F. Reviriego, *Magn. Reson. Chem.*, 2022, **60**, 442–451; (*b*) W. Zhang, X. Feng, Y. Zhou, J.-H. Chen, S. W. Ng and G. Yang, *Cryst. Growth Des.*, 2022, **22**, 259–268; (*c*) D. M. M. Krishantha, C. S. P. Gamage, Z. A. Schelly and H. V. R. Dias, *Inorg. Chem.*, 2008, **47**, 7065–7067.

22 Synthesis $Au_3(Pz^{Pr})_3$: K. Fujisawa, Y. Ishikawa, Y. Miyashita and K.-i. Okamoto, *Inorg. Chim. Acta*, 2010, **363**, 2977–2989; Synthesis $Au_3(Pz^{Ph})_3$: C. H. Woodall, S. Fuertes, C. M. Beavers, L. E. Hatcher, A. Parlett, H. J. Shepherd, J. Christensen, S. J. Teat, M. Intissar, A. Rodrigue-Witchel, Y. Suffren, C. Reber, C. H. Hendon, D. Tiana, A. Walsh and P. R. Raithby, *Chem. – Eur. J.*, 2014, **20**, 16933–16942; Synthesis $Au_3(Pz^{CF3})_3$: M. A. Omary, M. A. Rawashdeh-Omary, M. W. A. Gonser, O. Elbjeirami, T. Grimes, T. R. Cundari, H. V. K. Diyabalanage, C. S. P. Gamage and H. V. R. Dias, *Inorg. Chem.*, 2005, **44**, 8200–8210.

23 For selected references, see: (*a*) J. Lobo-Checa, S. J. Rodríguez, L. Harnández-López, L. Herrer, M. C. G. Passeggi Jr, P. Cea and J. L. Serrano, *Nanoscale*, 2024, **16**, 7093–7101; (*b*) S. Moyano, B. Diosdado, L. San Felices, A. Elduque and R. Giménez, *Materials*, 2021, **14**, 4550; (*c*) S. Moyano, J. L. Serrano, A. Elduque and R. Giménez, *Soft Matter*, 2012, **8**, 6799–6806; (*d*) C. Foces-Foces, I. Alkorta and J. Elguero, *Acta Crystallogr., Sect. B: Struct. Sci.*, 2000, **56**, 1018–1028.

24 A. I. Hanopolskyi, V. A. Smaliak, A. I. Novichkov and S. N. Semenov, *ChemSystemsChem*, 2020, **2**, e2000026.

25 All pK_a calculations were done using Chemicalize, [March, 2024], **https://chemicalize.com/**, developed by ChemAxon.

26 For cyclic trinuclear Au(I) complexes which show an eclipsed arrangement of trimers in the solid state, see: (*a*) C. Yang, M. Messerschmidt, P. Coppens and M. A. Omary, *Inorg. Chem.*, 2006, **45**, 6592–6594; (*b*) R. N. McDougald Jr, B. Chilukuri, H. Jia, M. R. Perez, H. Rabaâ, X. Wang, V. N. Nesterov, T. R. Cundari, B. E. Gnade and M. A. Omary, *Inorg. Chem.*, 2014, **53**, 7485–7499.

27 C. H. Woodall, S. Fuertes, C. M. Beavers, L. E. Hatcher, A. Parlett, H. J. Shepherd, J. Christensen, S. J. Teat, M. Intissar, A. Rodrigue-Witchel, Y. Suffren, C. Reber, C. H. Hendon, D. Tiana, A. Walsh and P. R. Raithby, *Chem. – Eur. J.*, 2014, **20**, 16933–16942.

28 (*a*) N. Eren, R. Svecova, F. Fadaei-Tirani, R. Scopelliti and K. Severin, CCDC 2453718 ($Au_3(Pz^{Ph})_2(Pz^{CF3})$): Experimental Crystal Structure Determination, 2025, DOI: **10.5517/ccdc.csd.cc2nc96k**; (*b*) N. Eren, R. Svecova, F. Fadaei-Tirani, R. Scopelliti and K. Severin, CCDC 2453719 ($Au_3(Pz^{Me})_2(Pz^{Ph})$): Experimental Crystal Structure Determination, 2025, DOI: **10.5517/ccdc.csd.cc2nc97l**; (*c*) N. Eren, R. Svecova, F. Fadaei-Tirani, R. Scopelliti and K. Severin, CCDC 2453717 ($Au_3(Pz^{Me})_2(Pz^{CF3})$): Experimental Crystal Structure Determination, 2025, DOI: **10.5517/ccdc.csd.cc2nc95j**; (*d*) N. Eren, R. Svecova, F. Fadaei-Tirani, R. Scopelliti and K. Severin, CCDC 2440472 ($Au_3(Pz^{CF3})_2(Pz^{Me})$): Experimental Crystal Structure Determination, 2025, DOI: **10.5517/ccdc.csd.cc2mxhxz**.